Charles University
Faculty of Mathematics and Physics

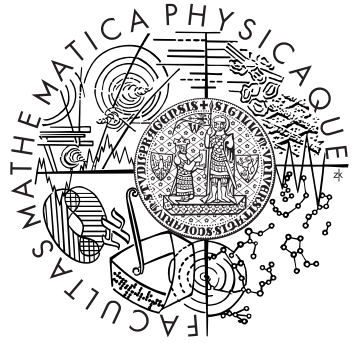

Josef Ďurech

Physical Models of Asteroids

HABILITATION THESIS

Prague 2016

Contents

1 Introduction

Asteroids are the most numerous objects in the Solar System and they carry information about the evolution of our cosmic neighbourhood. By studying their physical properties, we can learn a lot about the past and present processes that have formed our system. Asteroid research is an essential part of planetary sciences, it has even a recently emerging overlap to extrasolar systems.

Because asteroids are numerous and only few of them were visited by spacecraft for a detailed study, their research is in most cases limited to *remote sensing* data. These come in form of physical measurements of various properties. The analysis of remote sensing data is often connected with an *inverse problem*, i.e., a problem how to reconstruct the physical parameters of interest (shape, size, spin axis direction, surface properties,...) from measured data.

By applying inversion methods described in next sections to individual targets, their models are reconstructed. When a sufficiently large sample of models is available, we can study the distribution of physical parameters across the population (taking biases into account), look for correlations with orbital parameters, recover the evolution, etc.

Apart from the above-mentioned purely scientific motivation that drives asteroid research, there are two other aspects, more practical and often emphasized in public outreach. The first one comes from an inevitable fact that some of asteroids collide with Earth and a lot of effort is put to detecting potentially hazardous object. To be able to prevent a catastrophe, various deflection scenarios have been studied. No matter which of them will be eventually used, a good physical characterization of the object is needed before any deflection mission. So the role of remote sensing and modelling techniques is essential.

The second often mentioned practical aspect that has become more interesting in recent years, is the utilization of near-Earth asteroids (NEAs) as material resources. This is perhaps the most promising and exciting concept for the future – the observational and inversion techniques that have been developed for scientific purposes will be used for commercial aims (Kaasalainen and Ďurech, 2013).

In this thesis, I summarize my work on the problem of asteroid shape reconstruction. The main text is a compilation based on individual papers published over more that a decade. Those most important are included Sect. 7. Because the results are based on the *lightcurve inversion* method of Kaasalainen et al. (2001), I briefly review this method and the definition of the inverse problem in Sect. 2. The core of my work – the shape reconstruction of asteroids from disk-integrated photometry – is described in Sect. 3 together with the results regarding the distribution of asteroid spins. Then disk-resolved data, which provide detailed models, are described in Sect. 4. Three non-standard cases – binary asteroids, a non-constant rotation period, and an excited rotation – are discussed in Sect. 5. Directions for the future research are sketched in Sect. 6

2 Shape modelling of asteroids as an inverse problem

Historically, asteroids had been for a long time characterized by only six or seven numbers: six orbital elements and the absolute brightness that corresponds to the size. Because the brightness is proportional to the albedo that is in general unknown, the size is usually only an order of magnitude estimate (when only optical data are at hand).

Fortunately, asteroids do rotate and they do have non-spherical shapes, thus the amount of reflected light varies periodically with time – we observe a *lightcurve*. By observing asteroid lightcurves, we can thus almost directly measure their rotation periods. The measured synodic period is not constant because the asteroid moves relatively to the observer. What is more important for the spin axis determination is the change in shape of the lightcurves as the viewing and illumination geometry changes with both the asteroid and Earth orbiting Sun. The *forward problem* – predicting the brightness of an asteroid of a given shape and spin for a given time – is straightforward. The positions of Sun, Earth and the asteroid are known from ephemeris, the total reflected light is computed as a sum over individual surface elements. For nonconvex bodies, the shadowing has to be taken into account. However, both mathematically and astronomically more interesting is the *inverse problem* of how to reconstruct shape and spin axis direction from a set of lightcurves.

The history of using photometry as a source of information about asteroid shapes can be dated back to André (1901), who detected the light variations of (433) Eros caused by its rotation and elongated shape. Russell (1906) published a paper in which he showed that lightcurves can be caused by irregular shape, albedo variegation, or a combination of both and that the ambiguity between the shape and albedo cannot be broken for opposition geometry. The paper was rather discouraging in the sense that it showed that asteroid shapes cannot be derived uniquely for zero phase angles (opposition geometry). As shown much later by Kaasalainen et al. (1992b), this so-called *Russel degeneracy* is broken at moderate phase angles and is not problem for NEAs and main belt asteroids (MBAs) in practice.

With the availability of accurate photometric lightcurves, the pole orientations and shape parameters of asteroids were derived by using a model of triaxial ellipsoid. An overview of these older methods is given by Magnusson et al. (1989). These methods have one thing in common: they use only partial information from the lightcurves – amplitudes, times of extrema, for example – and then find a model that fits these *derived parameters* at best. This approach inevitably leads to loss of information. The complex information of a full lightcurve is reduced to few parameters. However, these methods gave important insight into pole orientation and elongation of asteroids.

Later Ostro and Connelly (1984) developed a method that derives a two-dimensional *convex profile* of a three-dimensional body, which was a mid-step towards the full 3-D convex inversion. The general inversion method was first introduced by Kaasalainen et al. (1992b,a) and a practical scheme was developed by Kaasalainen and Torppa (2001) and Kaasalainen et al. (2001). This method or its modification was then used for most of the shape models reconstructed from photometry and is briefly described below.

2.1 Parametrization of the model

Asteroids are assumed to be solid bodies that rotate around a fixed-in-space rotation axis with a constant sidereal rotation period P. The orientation of the rotation axis in the inertial frame is described by the ecliptic longitude λ and latitude β of the spin vector direction. The "sense" of rotation is defined by the right-hand rule. The angle between the spin axis and the normal to the orbital plane is called *obliquity* ε. The spin parameters λ, β, and P together with the initial rotation angle φ_0 at some epoch JD_0 uniquely define the orientation of the asteroid in space for any given time.

In reality, some asteroids do not rotate in the principal axis mode. Their rotational state can be described as force-free precession, which is discussed in Sect. 5.1. The case of a non-constant rotation period is discussed in Sect. 5.2.

2.1.1 Convex shapes

A *convex* shape model is a mathematical approximation to real shapes of asteroids, which are generally nonconvex on scales from the global nonconvexity to macroscopic roughness. Intuitively, one would expect that given the (sometimes highly) nonconvex shapes of real asteroids (revealed by spacecraft), convex shapes would be only a poor approximation. Contrary to this expectation, convex models give a surprisingly good fit to lightcurves and other disk-integrated data of asteroids, even for those that were proven to be highly nonconvex or even binary. This means that there is very little need for nonconvex models derived from disk-integrated photometry. If convex models fit the data generally very well down to the noise level, nonconvex models cannot fit the data better. And we cannot distinguish from the goodness-of-fit which model is better. More over, a convex solution is mathematically unique, robust against data noise, and requires only weak regularization of albedo homogeneity.

A convex shape is represented by areas s_i of surface facets and corresponding normals $\vec{n}_i$. The normals are fixed while the ares are optimized to get the best agreement between the model brightness and the data. The distribution of individual areas is usually parametrized by spherical harmonics. The advantage of this approach is that the only regularization needed is to make the set of facets a closed surface, i.e, the condition $\sum_i s_i \vec{n}_i = 0$ has to be fulfilled. The set of normals and corresponding areas represent so called *Gaussian image*, from which the polyhedral model is reconstructed by *Minkowski minimization* (Kaasalainen and Torppa, 2001).

The convex inversion method has been widely used and its reliability was confirmed by comparison of its results with independent methods (Kaasalainen et al., 2005; Marchis et al., 2006; Ďurech et al., 2011; Keller et al., 2010, for example). The output of the lightcurve inversion method is a shape model represented by a convex polyhedron that approximates the real nonconvex shape of an asteroid. Because of the general coupling between the size and albedo, the models are scale free. They can be set to scale by disk-resolved data, stellar occultation silhouettes, of thermal infrared data.

2.1.2 Nonconvex shapes

From a modelling point of view, the step from convex to nonconvex shapes is straightforward – instead of optimizing surface areas of the corresponding Gaussian image of a convex model, we will parametrize the nonconvex shape directly. For example, we can represent a nonconvex surface by a radius vector $r(\vartheta, \varphi)$ for each direction defined by spherical coordinates ϑ, φ. In practice, r is discretized by defining a triangular grid approximating the smooth surface. The real shape is then approximated by a nonconvex polyhedron. The parameters of optimization are the lengths r directly, or they are expressed in terms of spherical harmonics, and the parameters to be optimized are the coefficients of the spherical harmonics expansion.

The shapes that can be described by $r(\vartheta, \varphi)$ are necessarily starlike. However, not all asteroids are regular enough to be described by this parametrization. To be able to work with shapes that are non-starlike, Viikinkoski et al. (2015a) introduced other parametrizations, namely the so-called octantoids and subdivision control points.

2.2 Inversion

In practice, the optimization starts from some point in the parameter space and converges (using the Levenberg-Marquardt algorithm, for example) to the local minimum. The conversion in shape parameters is robust, i.e., it does not depend on the initial values of parameters, thus the initial shape is usually a sphere. For the pole direction, there are typically only a few local minima on a sphere, thus it is sufficient to start at about ten positions about isotropically covering the unit sphere. A completely different situation is in the case of period, where local minima are densely packed and similar values of the rotation period can correspond to very different values of the pole direction and shape. The determination of the correct sidereal rotation period is crucial for the whole inversion and one has to make sure that the global minimum is found. This is in practice done by running the optimization from different initial points in the period parameter space.

2.3 Regularization and stability

As with almost any inverse problem, issues related to stability of the solution and regularization arise. In case of convex models, the original formulation of the problem of finding areas of surface facets is linear, because the amount of reflected light is directly proportional to the area. However, the areas have to be positive, which is in practice done by substituting the original parameters s_i by $s_i = \exp p_i$, which makes the parameters s_i positive but causes the problem to become nonlinear in p_i. The only regularization needed is that the condition $\sum_i s_i \vec{n}_i = 0$ has to be fulfilled to make the set of areas closed (see Sect 2.1.1). Formally, this is done by a dark area that makes this condition true and that does not correspond to the reflected light. When this area is large compared to the whole surface, it may indicate that the assumption about the uniform albedo is not valid.

In case of nonconvex models, the situation is different, because now the problem is a typical ill-posed inverse problem that is sensitive to data noise, light-scattering model, resolution, etc. Therefore, various regularizations are needed. The obvious one is regularization against too irregular shapes with spiky features. This is done by penalizing solutions with large differences between normals of adjacent facets. Another regularization is that the body has to rotate along the axis with the maximum moment of inertia (assuming uniform density). Again, deviations from this rotation are penalized.

In general, nonconvex models require more regularization than convex ones and the results depend on the particular weights of these regularizations. When producing a nonconvex shape model, one should ideally estimate also the uncertainties of the shape not only with respect to random and systematic errors in the data, but also with respect to the parametrization of the model. Thus different shape parametrizations reveal which shape features are likely to be real and which are only artifacts of modelling.

2.4 Inversion codes

The original inversion code of Mikko Kaasalainen was re-written from Fortran to C by me, slightly modified, and made public. It is available through the Database of Asteroid Models from Inversion Techniques (DAMIT).[1] Apart from the widely used version that uses spherical harmonics representation (`convexinv`), there is also the code that uses directly surface areas as parameters (`conjgradinv`) and also the code for the forward problem (`lcgenerator`). The code was used not only by our group, but also by others to reconstruct asteroid shapes from photometry (Marciniak et al., 2011; Apostolovska et al., 2014; Polishook, 2014; Silva and Lazzaro, 2015, for example).

Through DAMIT, we also released the All-Data Asteroid Modelling (ADAM) code (Viikinkoski et al., 2015a), that is suitable for inversion of lightcurves combined with disk-resolved images, radar delay-Doppler echoes, or interferometric data (Viikinkoski et al., 2015b).

[1] `http://astro.troja.mff.cuni.cz/projects/asteroids3D/web.php?page=download_software`

3 Disk-integrated data

Due to small angular size of most of asteroids, they are (apart from the largest ones) point-like sources and the detected flux in optical or infrared wavelengths is integrated over the whole disk facing the observer. Thus, for most asteroids, the *disk-integrated data* are the only type of data we can get. The level of detail we can reconstruct from disk-integrated data is inevitably smaller than when using disk-resolved data, but their availability for hundreds of thousand asteroids makes this source the most important one.

3.1 Photometry

Photometry has been and likely will remain the most important source of information about asteroids, because it is to some extent available for every known object. The brightness variations caused by rotation and irregular shape (albedo variegation is much less important) carry information about the rotation period, the spin axis orientation, and the shape. If the sampling is dense with respect to the rotation period, we measure a *lightcurve*. By estimating the period of a lightcurve, we directly measure the rotation period of an asteroid. At present, the largest database of asteroid periods (Warner et al., 2009) contains data for almost 17,000 asteroids, from which about 4,000 have the period determined reliably and unambiguously.[2] When an asteroid is observed from different viewing geometries (which requires several apparitions for a main-belt asteroid), the lightcurve inversion can be applied and a unique solution of the inverse problem can be found. This way, hundreds of shape models ware derived, most of them by our group.

Another type of photometry comes from surveys, which typically image large portion of the sky each night with low cadence. Thus the rotation period of a typical asteroid (hours) is sampled very sparsely and we call this *sparse photometry*. Over years, a survey collects hundreds of points for most of the observed asteroids. After Kaasalainen (2004) had shown that these data can be used the same way as standard lightcurves, we used sparse data to significantly increase the number of shape models (Ďurech et al., 2005, 2007, 2009; Hanuš et al., 2011, 2013b; Ďurech et al., 2016). Although the photometric accuracy of currently available data is low, the large number of data points makes sparse photometry a rich source of information about asteroid shapes.

3.1.1 Period search for sparse data

The lightcurve inversion method uses a gradient-based algorithm to converge to the local minimum in parameter space. The local minima in the period subspace are densely packed with a typical separation of $0.5P^2/\Delta T$, where P is the rotation period and ΔT is the interval covered by observations. This corresponds to the shift in phase of half the rotation (Kaasalainen, 2004). In case of dense lightcurves, the situation is easy because a very good estimate of the sidereal period is given by the Fourier analysis of the lightcurves (assuming two-peak lightcurves). The period search is then ran in a relatively narrow interval around this value. A different situation is when only sparse data are available – then we do not have any information about the rotation period, because Fourier analysis cannot be successfully used.

Period scans are time-consuming when any a priori information about the rotation period is not available and the scanned interval is large. To increase the speed, it is possible to use a simplified model – a geometrically scattering ellipsoid, for example (Kaasalainen and Ďurech, 2007). The main advantage of this simple model is that the amount of scattered light can be computed analytically (Connelly and Ostro, 1984), which makes the period search about hundred times faster than with convex shapes. Although the ellipsoid model is quite simple and the geometrical scattering is not physical, this approach serves very well for the initial period scan. The period found with ellipsoids can be then used as a start point for the full convex inversion.

An example of the periodogram for a model using ellipsoids and for full convex modelling is shown in Fig. 1 for asteroid (136) Austria. Both methods found the correct rotation period of $\sim$ 11.5 h (known from dense lightcurves), which gives the lowest residual. However, it is not always

[2] `http://www.minorplanet.info/lcdbquery.html`

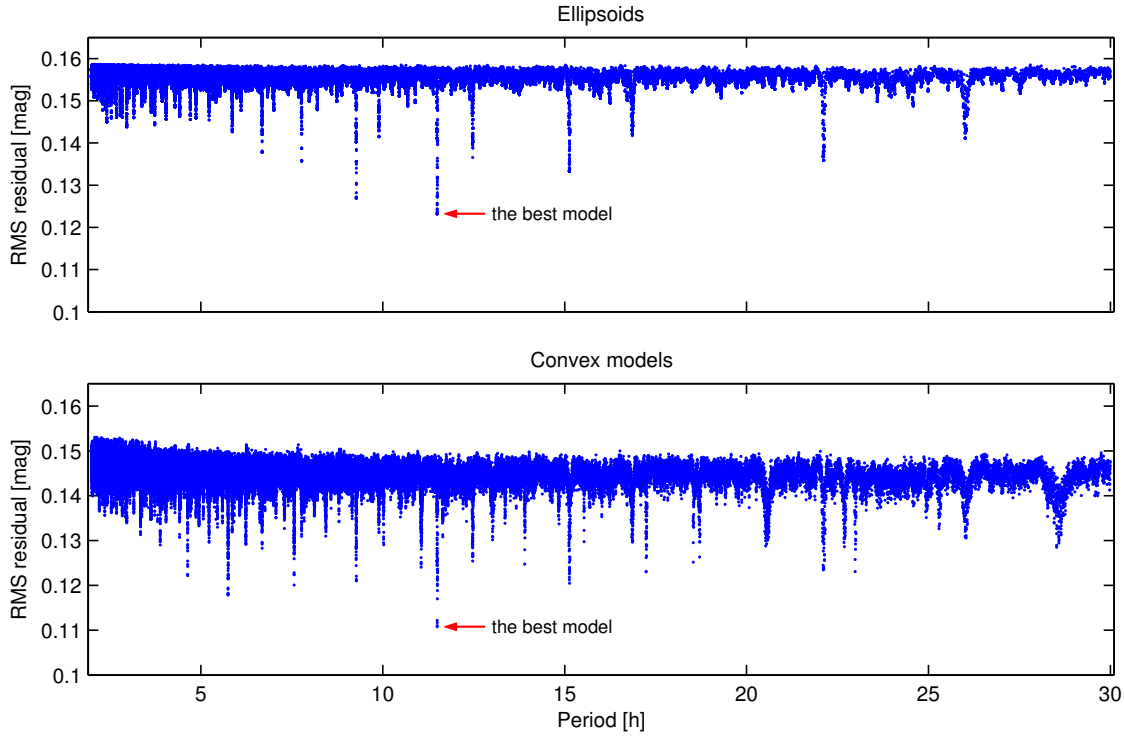

Figure 1: Period search using ellipsoids (*top*) and convex models (*bottom*). The periodograms were computed for sparse data from Lowell Photometric Database for asteroid (136) Austria.

clear if the solution corresponding to the lowest residual is a unique one – in other words, if the global minimum is deep enough with respect to other local minima. The definition of uniqueness of a model is perhaps the main practical problem, because the size of errors of data and their distribution are not exactly known, thus standard χ^2-based approach cannot be used because it usually leads to unrealistically small error intervals and consequently to false positive solutions.

The sparse data have become the most important source of photometry. Although their poor photometric quality of ~ 0.1 mag, they can be successfully inverted for high-amplitude asteroids. More over, they can be combined with dense lightcurves that define the rotation period. The most promising source of sparse data is the Lowell Photometric Database (Bowell et al., 2014). To be able to effectively process this database that contains data for hundreds thousands of asteroids, we set up a distributed computing project Asteroids@home.

3.1.2 Asteroids@home

It is a distributed computing project built on the Berkeley Open Infrastructure for Network Computing (BOINC) – a platform that has been developed for SETI program. We used the `convexinv` code and modified it to fulfill BOINC specifications (Ďurech et al., 2015). During the test phase, we cooperated with experts on distributed computing projects from the Czech National Team.[3] The BOINC server also enables credits to be given to users, discussion forum, ranking, and other features that are important for motivation of volunteers.

For each asteroid, the original wide search interval (typically 2–100 hr) is divided into small units that are distributed among volunteers. The results are then cross-validated and joined together. The preliminary results are published on the web of the project (`http://asteroidsathome.net`), models of asteroids are then validated and published in peer-reviewed journals (Ďurech et al.,

[3] `http://www.czechnationalteam.cz`

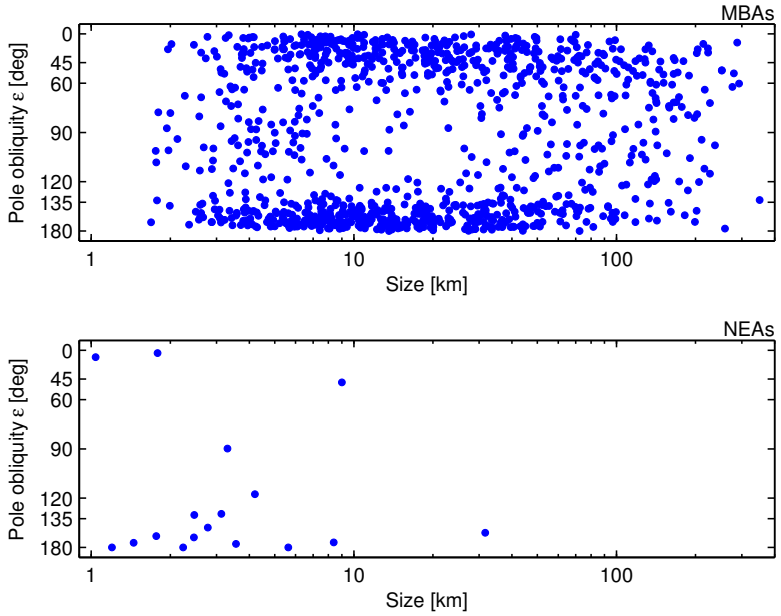

Figure 2: The distribution of pole obliquity ε as a function of size for main-belt (*top*) and near-Earth asteroids (*bottom*). The scale on the ordinate is such that an isotropic distribution of spins would be uniform distribution in this plot. If there are two possible models for an asteroid, the mean value of obliquities for the two models is plotted.

2016). The number of volunteers is huge and still growing, there have been more than 75,000 people with 130,000 computers connected to the project; the total computational power is about 250 TFLOPs, making Asteroids@home one of the top-ten currently active distributed computing project.

Apart from scientific results, this platform is also ideal for public outreach, because the volunteers are directly connected with the scientific research. The project significantly contributed to the increase of asteroid spin/shape models.

3.1.3 Statistics of poles

It has been long known that the distribution of spin directions of asteroids is not isotropic (Kryszczyńska et al., 2007, for example). With increasing number of asteroid models, the statistics of pole directions has become more robust. With about 900 asteroids in DAMIT and other $\sim$ 300 unpublished model based on Lowell and WISE data (Ďurech et al., in prep.), we have a large sample to study how the distribution of spins depends on other parameters. A strong dependence on size is shown in Fig. 2 for main-belt and near-Earth asteroids. Instead of the pole ecliptic longitude β, I plot the pole obliquity ε, which for asteroids orbiting close to the ecliptic plane is $\varepsilon \approx 90^\circ - \beta$.

The lack of smaller asteroids with poles close to the ecliptic ($\varepsilon \sim 90^\circ$) was explained by Hanuš et al. (2011) as YORP-induced evolution of spins (Hanuš et al., 2013b). Extreme obliquities are end-states of YORP evolution. More over, the distribution of obliquities is not symmetric around 90° (Fig. 3). As already noticed by Hanuš et al. (2013b), the retrograde rotators are more concentrated to $\varepsilon \sim 180^\circ$, probably because prograde rotators are affected by resonances. For larger asteroids, there is an excess of prograde rotators that might be primordial (Kryszczyńska et al., 2007; Johansen and Lacerda, 2010).

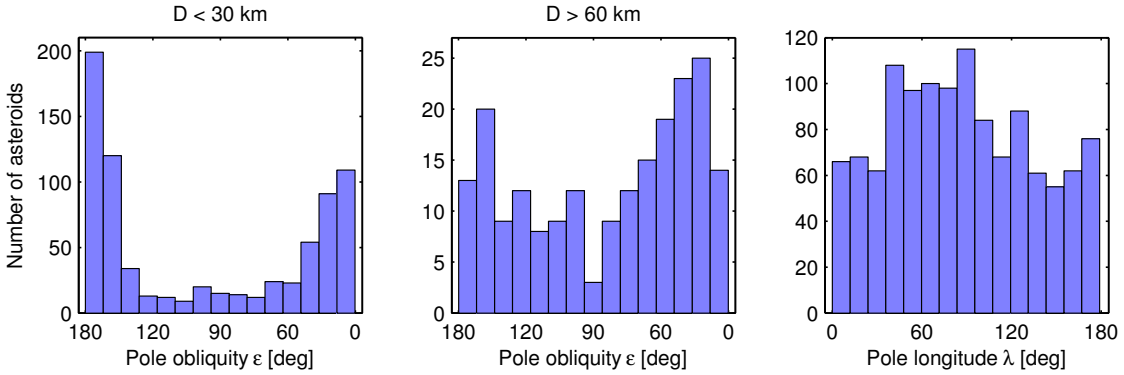

Figure 3: Histograms of distribution of pole obliquities ε for asteroids with diameters < 30 km (*left*) and > 60 km (*middle*), respectively and a histogram of distribution of pole longitude λ for all main-belt asteroids (*right*).

The excess of retrograde rotators among NEAs (Fig. 2) can be explained by the Yarkovsky-induced delivery mechanism from main belt through resonances (La Spina et al., 2004), although the number of NEA models in our sample is too small for any reliable statistics.

The plots shown here do not take into account the bias in the data and the method, so the real distribution of an unbiased sample would be different. Because most of the models are based on noisy sparse data, there is a strong selection effect towards elongated bodies with large lightcurve amplitude for which the signal is not drowned in the noise. However, the biases are in general significantly lower than the features we see in Figs. 2 and 3. The lightcurve inversion is less efficient for asteroids with poles close to the ecliptic plane but the bias in the method is of the order of tens percent (Hanuš et al., 2011; Santana-Ros et al., 2015) and cannot explain the significant "gap" for obliquities between 60–120°. Proper debiasing will be the next important step on the way to reveal the distribution of spins in the asteroid population, their dependence on the size or other physical properties, and their distribution in different dynamical or taxonomical subpopulations.

Apart from pole obliquity, which is closely related to the pole ecliptic latitude β, we can also study the distribution of pole longitudes λ. In Fig. 3, we see a clear deviation from a uniform distribution of pole longitudes. Because of ambiguity in pole direction – there are often two solutions with similar latitudes and difference in longitudes of about 180° – the distribution is plotted modulo 180°. The histogram shows a statistically significant excess of asteroids with λ around 50–100°. This was already announced by Bowell et al. (2014), who processed the Lowell data set by a different approach, estimated spin-axis longitudes for more than 350,000 asteroids, and revealed an excess of longitudes at 30–110° and a paucity at 120–180°. Contrary to satisfactorily explained YORP-driven distribution in ε, the explanation of this phenomenon in λ remains unclear.

3.1.4 Spin distribution in asteroid families

The YORP evolution of spins is also present in asteroid families (Fig. 4). Because Yarkovsky drift in semimajor axis is proportional to $1/D^2$, where D is the size of an asteroid, smaller asteroids are transported more effectively – they move faster. This explains the typical "V-shape" of asteroids families when their members are plotted in proper semimajor axis a_{p} vs. size approximated by the absolute magnitude H. After its origin, a family was located near its current center and then it evolved in time such that smaller asteroids (higher H) moved farther away from the centre of the family. Because the direction of the Yarkovsky drift depends on the orientation of the spin axis – prograde rotators drift outwards, retrograde inwards – we expect a nonrandom distribution of spins for left and right "wings" of the family. Indeed, this is what we observe for members of families. Two examples are shown in Fig. 4. The Flora family, whose left part was removed by

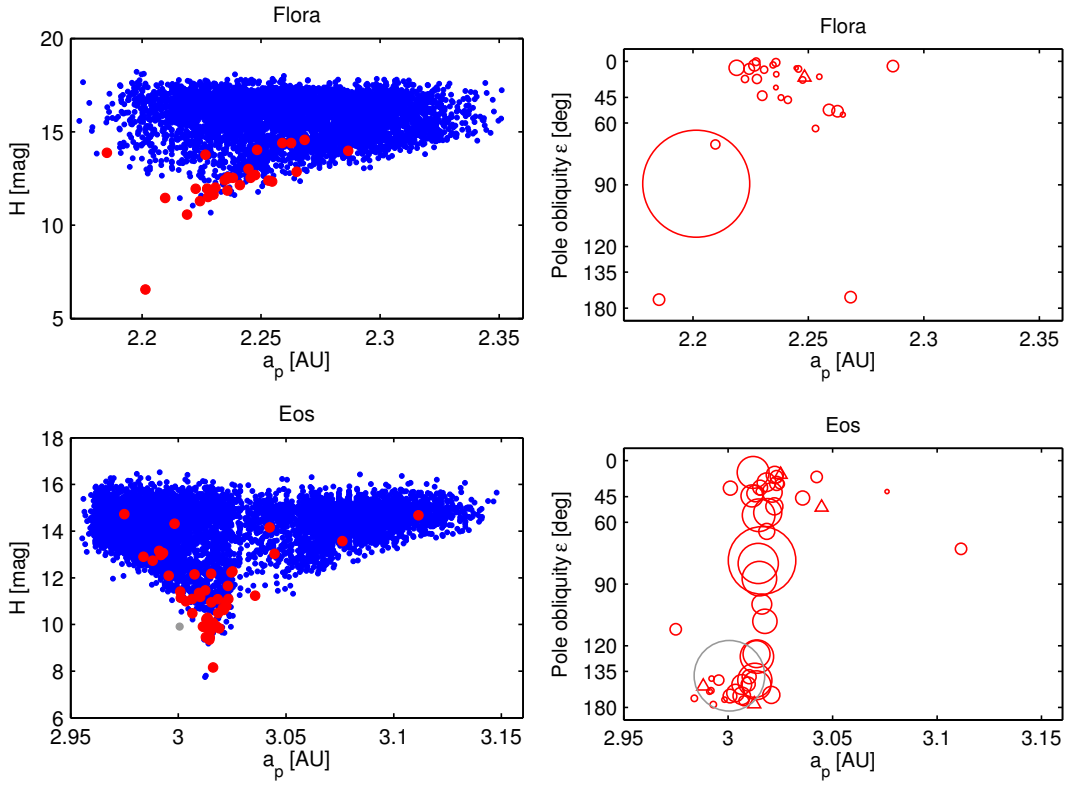

Figure 4: Spin distribution in Flora (*top*) and Eos (*bottom*) asteroid families. Left panels show the distribution of all (*blue*) members of the family in the proper semi-major axis $a_{\rm p}$ vs. absolute magnitude H, the asteroids for which we have a model are in red. The right panels show the distribution of obliquities for family members with a model. The sizes of the circles are proportional to the size of the asteroid. The triangles mean that the size is not known. The grey asteroid in Eos family is likely an interloper.

the ν_6 resonance, has almost all members for which we have a model on the right from the center and rotating in the prograde sense. A similar behaviour is shown also for Eos family.

The knowledge of spin orientation of asteroids in families can be in principle used for dating those families. To do so, we would have to know YORP timescales to be able to say how fast the spin reorientation is and how efficient is the so-called stochastic YORP (Bottke et al., 2015). A lot of information is still missing, because usually we have information only about the largest members of each family.

3.1.5 Distribution functions

The number of models will inevitably always lack behind the number of known asteroids – just because it takes time to collect enough data for an asteroid. So an alternative approach of modelling directly the *distribution of physical parameters* instead of reconstructing this distribution from individual models would be more effective. The first attempt was done by Szabó and Kiss (2008), who analyzed Sloan Digital Sky Survey (SDSS) data of asteroids and detected different elongation of asteroids in different families. They interpreted this as an evolution of shapes from elongated to spheroidal due to impacts. However, our re-analysis of the same SDSS data and a mathematical analysis of the problem (Nortunen and Kaasalainen, 2016) is in contradiction with their results.

Contrary to lightcurve inversion when the best model is such that has the best fit to the brightness, the alternative approach computes some observables that are then fitted by a population. From various observables that can be derived from brightness–time pairs, the mean brightness and its variance are robust and can be used for inversion (Nortunen and Kaasalainen, 2016). Asteroids are characterized only by the pole latitude β and shape elongation $p = a/b$, where $a, b = c = 1$ are semiaxes of an ellipsoid. Using this simple shape model and assuming geometrical scattering and opposition geometry, the brightness can be computed analytically and the inverse problem is fast. By analyzing the change of mean brightness, Bowell et al. (2014) discovered an unexpected non-uniformity in the distribution of pole longitudes. Our independent analysis of the same data set with a different approach using not only the mean brightness but also the dispersion of brightness (Cibulková et al., in prep.) confirm this result. More over, the distribution in λ is about the same as that based on models from lightcurve inversion (Fig. 3).

This new approach of working with distribution functions instead of individual models opens a new possibility for data exploration. Both theoretical analysis of the problem and practical test with real data (Nortunen et al., in prep.) show that we can unambiguously reconstruct the distribution of β and p from current surveys.

3.2 Thermal infrared data

Apart from reflected light in visual or near-infrared wavelengths, asteroids emit also thermal radiation in infrared (IR) wavelengths. Measured IR fluxes have been used for determining the sizes of asteroids, because – contrary to reflected light – thermal radiation is not sensitive to (unknown) reflectivity of the surface. When accurate IR data are available, they can be used to derive thermal properties of the surface. This is done by using so called *thermophysical model* (TPM), which computes the distribution of the temperature on the asteroid surface (by solving the 1-D heat diffusion problem) and then computes the corresponding thermal flux from the surface. The thermophysical models include different levels of simplification, the most advanced try to realistically model the self-illumination and self-heating of a rough surface (for a review see Delbo et al., 2015).

When interpreting thermal data and using a thermophysical model, the shape and spin state of the asteroid have to be known to enable computing the viewing and illumination geometry for each facet on the surface (and shadowing in case of a nonconvex model). Traditionally, the thermophysical models were used in combination with a fixed shape and spin that were taken from a radar- or a lightcurve-based model. Although this approach in general works and provides reliable thermophysical parameters, the main caveat here is that usually the uncertainties of the shape and spin state are not taken into account. We have shown that this may lead to underestimation of errors of the derived parameters or even erroneous results (Hanuš et al., 2015).

To over come the problem of two-step modelling, we incorporated TPM into convex shape lightcurve inversion (Ďurech et al., 2012). The new approach models everything at once. We use the lightcurve inversion method where, apart from reflected light, the temperature of each facet is computed and then the corresponding thermal flux. Our new code joins two widely used and well tested methods: (i) the lightcurve inversion of Kaasalainen et al. (2001) and (ii) the thermophysical model of Lagerros (1996, 1998). We use the convex approach, which enables us to work in the Gaussian image representation: As we work with convex shapes only, shadowing plays no role, although the generalization of the problem to nonconvex shapes is straightforward, similarly as in case of lightcurve inversion.

For computing the brightness of an asteroid, we use Hapke's model with shadowing (Hapke, 1981, 1984, 1986). This model has five parameters: the average particle single-scattering albedo ϖ_0, the asymmetry factor g, the width h and amplitude B_0 of the opposition effect, and the mean surface slope $\bar{\theta}$. Contrary to standard TPM methods where the size of an asteroid and its geometric albedo are connected via the Bond albedo, phase integral, and absolute magnitude, we use a self-consistent approach based on Hapke's model. The problem is that Bond albedo as well as visual geometric albedo are not material properties and they are unambiguously defined only for a sphere. In our approach, the total flux scattered towards an observer is computed

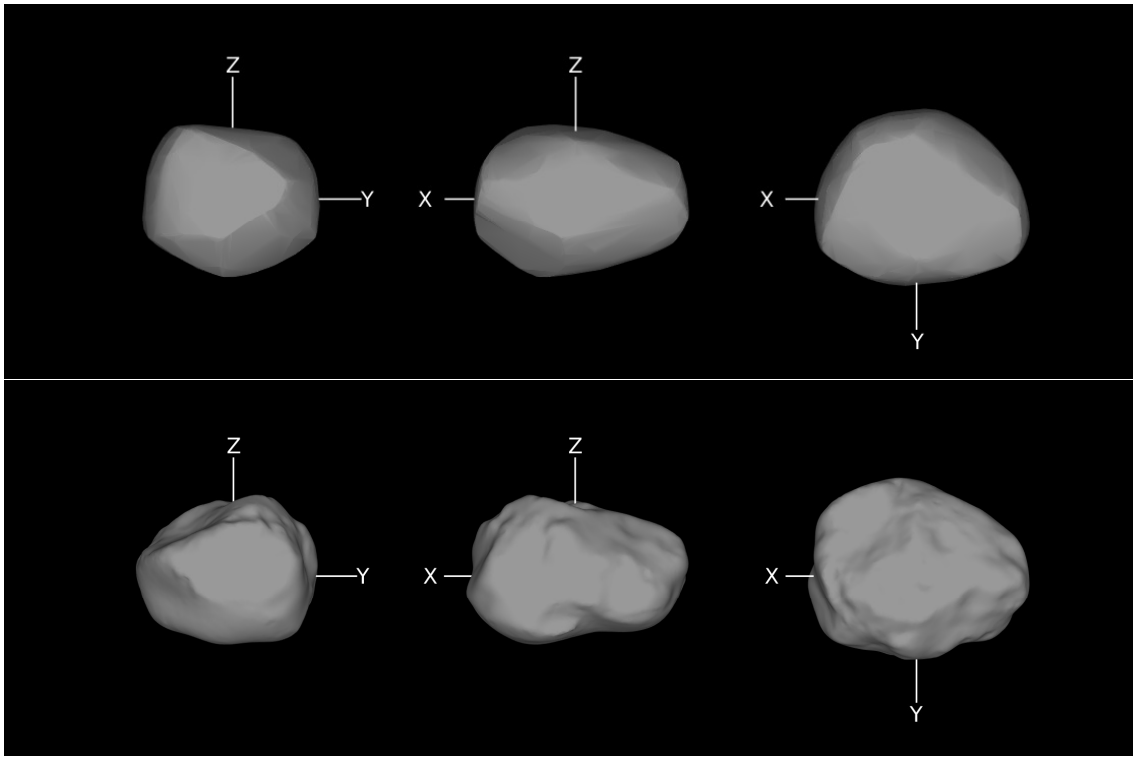

Figure 5: Comparison between the shape of (21) Lutetia reconstructed by our method of inversion of optical and thermal data (*top*) and that reconstructed by Sierks et al. (2011) from Rosetta fly-by images (*bottom*).

as a sum of contributions from all visible and illuminated facets. Hapke's parameters are also used to compute the total amount of light scattered to the upper hemisphere, which defines the hemispherical albedo needed for computing the energy balance between incoming, emitted, and reflected flux.

Parameters of the thermophysical model are the thermal inertia Γ, the fraction of surface covered by craters and their opening angle. To find the best-fit parameters, we use the Levenberg-Marquard algorithm. The parameters are optimized to give the lowest value for the total χ^2 that is composed from the visual and infrared part weighted by w:

$$\chi^2_{\mathrm{total}} = \chi^2_{\mathrm{VIS}} + w\chi^2_{\mathrm{IR}}\,.$$

The weight w is set such that there is a balance between the level of fit to lightcurves and thermal data. Objectively, the optimum value can be found according to the method proposed by Kaasalainen (2011).

As an example of how well the thermal and optical data together can determine the shape model, I show in Fig. 5 a convex model of Lutetia reconstructed from disk-integrated lightcurves and thermal data and a detailed shape reconstructed from Rosetta fly-by imaging (Sierks et al., 2011) that serves as a ground-truth for comparison with our model. The volume-equivalent diameter of Rosetta-based model is 98 km, while our model has diameter of 103 km. The thermal inertia $\Gamma = 20\,\mathrm{J\,m^{-2}\,s^{-0.5}\,K^{-1}}$ agrees well with the value $\Gamma < 20$–$30\,\mathrm{J\,m^{-2}\,s^{-0.5}\,K^{-1}}$ by Keihm et al. (2012).

We applied this method to asteroid (162173) Ryugu, the target of JAXA Hayabusa 2 sample-return mission. Although the low quality and small amplitude of optical lightcurves did not allow us to uniquely reconstruct the shape, we constrained the size, thermal inertia, albedo, and most importantly the pole direction of this asteroid (Müller et al., in prep.).

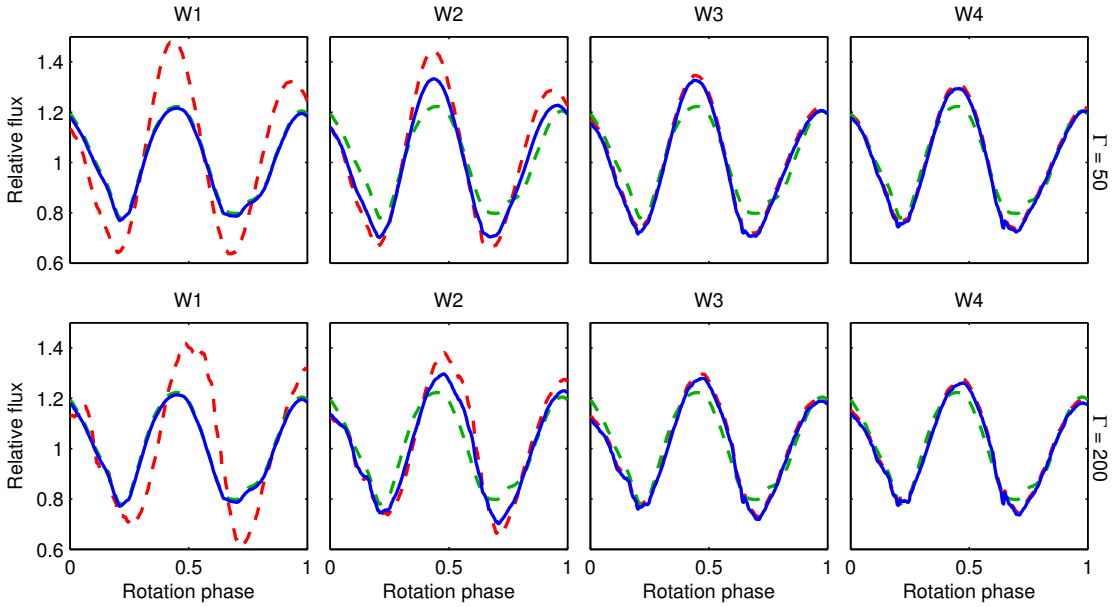

Figure 6: Comparison of normalized reflected and thermal emitted flux for shape model of (3767) DiMaggio in four WISE filters. The green dashed curve on all subplots is the classical lightcurve in reflected light. The solid blue curve is the total flux that is composed from reflected (green curve) and emitted (dashed red curve). All curves are normalized such that their mean flux is 1. The ratio between reflected/emitted is high for W1, W2 filters and almost zero for W3 and W4 filters. The fluxes were computed for two values of thermal inertia $\Gamma = 50$ (*top*) and $200\,\mathrm{J\,m^{-2}\,s^{-1/2}\,K^{-1}}$ (*bottom*) using the derived model of DiMaggio and the geometry corresponding to WISE observations (Ďurech et al., 2016).

3.3 Thermal infrared data as reflected light

The approach described above has an enormous potential to combine optical and thermal data that are now available for tens of thousand of asteroids. However, the problem of finding a unique period in sparse data with full TPM is very time consuming and the only way how to handle it is to use distributed computing. We plan to include thermophysical modelling into our Asteroids@home project.

Meanwhile, we also tested an alternative approach of using thermal data without any TPM for period determination. The Wide-field Infrared Survey Explorer mission (Wright et al., 2010) observed asteroids during its cryogenic mission in four filters (denoted W1, W2, W3, and W4) at wavelengths 3.4, 4.6, 11, and 22 μm, respectively (Mainzer et al., 2011). While W3 and W4 fluxes consist of almost entirely thermal flux and have been used in thermophysical models of selected asteroids (Alí-Lagoa et al., 2014; Rozitis et al., 2014; Hanuš et al., 2015, for example), the W1 and W2 filters are mixture of reflected and emitted flux. The sampling of WISE data is typically about ten points per filter in a day or two, which makes them semi-sparse, a compromise between the densely sampled lightcurves and sparsely sampled photometry from surveys.

According to our tests (Ďurech et al., 2016), the WISE data in all filters can be treated as reflected light (see Fig. 6) if the aim is to find the correct rotation period, because the shapes of lightcurves in different filters are similar and absolute scaling is not important. WISE data are available for tens of thousands of asteroids, so this is a potentially rich source of new asteroid models.

4 Disk-resolved data

Contrary to disk-integrated data, disk-resolved data provide us with shape details that can be used to reconstruct general concave models of asteroids without the limitation to convex shapes. However, disk-resolved data are available for only a small fraction of asteroids.

4.1 Adaptive optics

Most of asteroids are too far and to small to be more than point-like sources for current instruments. However, some of the largest asteroids have been resolved either with the Hubble Space Telescope (HST) or with ground-based telescopes equipped with adaptive-optics (AO) systems. The achievable angular resolution of 30 mas corresponds to $\sim$ 40 km at 2 AU from Earth, which is sufficient for resolving disks of the largest main-belt asteroids and even providing some details of their surface. With new instruments (SPHERE/VLT), the resolution is even better enabling to potentially resolve hundreds of MBAs.

The process of AO observations is more than simple imaging, it also includes deconvolution of raw images. Ideally, one could fit the observed AO image with the model prediction. However, the deconvolved images often show artificial details that are products of processing, not the real features on asteroids. More over, the brightness distribution on the disk is a function of light-scattering parameters that are in general unknown and have to be modelled. For these reasons, the comparison between the model and the data is not done for the whole image but only for the boundary. From an AO image, the contour of the disk is at first extracted and this is then compared with the contour of the model. As has been shown by Kaasalainen (2011), the boundary curves have the same information content as the full images. The contours can be used for shape reconstruction (Merline et al., 2013; Berthier et al., 2014, for example) or for scaling convex models (Hanuš et al., 2013a)

This approach involves one step that is sensitive to a particular setup – the contour extraction. There are many ways how to define the contour of a pixelized image and it is not clear which one is mathematically the best. More over, the definition of a contour or a boundary becomes poorly defined with only a few pixels resolution. To overcome these problems, Viikinkoski et al. (2015a) came up with an alternative approach that does the model vs. observation comparison not in the space domain of an AO image but in its Fourier transform. This way, all data are used but the inner part of the image has less weight because the Fourier transform stresses out edges and there is no need to define the boundary. More over, the Fourier domain is natural for interferometric data (see Sect. 4.2). We applied this approach for the first time to asteroid (3) Juno (Viikinkoski et al., 2015b)

4.2 Interferometry

The concept of inversion of interferometric data can be formulated in the framework of generalized projections (Kaasalainen and Lamberg, 2006). The first example of using interferometry of asteroids for inversion was the processing of HST Fine Guidance Sensor data (Hestroffer et al., 2002; Tanga et al., 2003). Another example is a model of binary asteroid (939) Isberga reconstructed from lightcurves and mid-infrared interferometry by Carry et al. (2015).

At present, the main interferometric instrument is the Atacama Large Millimeter Array (ALMA). This facility currently provides baselines up to 12.6 km at frequencies up to 230 GHz, which corresponds to angular resolution of 30 mas. This is about the same resolution as with AO but should be significantly better ($\sim$ 7 mas) when the highest frequencies will be available for the longest baselines. The frequencies at which ALMA observes correspond to wavelengths of thermal emission. Thus, for the forward problem and for the inverse as well, one would need to solve the heat diffusion problem similarly as in Sect. 3.2. However, because with ALMA we have disk-resolved data, the information content is dominated (similarly as in case of AO images) by the boundary data where the contrast is at maximum, so the actual distribution of the temperature across the disk is not so important and we can use a much simpler and computationally faster model of

Vokrouhlický and Nesvorný (2008). This way, the first test of inverting ALMA data was done by Viikinkoski et al. (2015b) with the ADAM code.

4.3 Occultations

Another technique that can be used for asteroid shape reconstruction is to observe stellar occultations by an asteroid. The projected shadow that crosses the Earth surface can be measured by measuring timings of the star disappearing and reappearing from the shadow. The success of this methods depends critically on the number of observers (thus the points on the projection), their distribution across the path of the shadow, and the accuracy of timings (that has to be better than 0.1 s). The main advantage of this method is that it is not dominated by the brightness of the asteroids, thus is not limited to only angularly large asteroids (as the previous methods), and is applicable also on trans-Neptunian objects (TNOs). This area is a domain of amateur astronomers and their importance will further increase with the final catalogue of the Gaia mission that will enable to make the predictions more accurate (Tanga and Delbo, 2007).

Occultations can be used to directly measure asteroids diameters. If no information about the shape is known, the orientation of the body for the time of occultation is not known and the projected silhouette gives only a lower limit for the size. On the other hand, if there is a model from lightcurves, we can predict its orientation and scale it to give the best fit with the occultation timings. This way, we scaled shape models of many asteroids and solved pole ambiguity for some of them (Ďurech et al., 2011).

When there are many observers placed in the path of the shadow and the timings are precise, the silhouette of the asteroid is well defined and the points can be used a similar way as AO images for shape reconstruction. An example is shown in Sect. 5.3.

5 Nonstandard cases

In the previous sections, an asteroid was modelled as a single body rotating with a constant spin vector. However, some asteroids exhibit complex rotation, some show changes in their rotation rate, and a significant part of the population of small bodies is composed of binary systems. In some sense, these – from the point of view of inversion – "nonstandard" cases are more interesting than "standard" ones because they are more complex.

5.1 Excited rotation

Although most asteroids for which we have photometric data show strictly periodic variation of their lightcurves, which corresponds to a relaxed rotation, some asteroids exhibit quasi-periodic lightcurves that can be interpreted as produced by a body that is in an *excited* (also called *tumbling*) *rotation state*. The first model of a tumbling asteroid was created by Hudson et al. (2003) for asteroid (4179) Toutatis from radar data. From optical lightcurves, we reconstructed models of 2008 TC_3 (Scheirich et al., 2010) and (99942) Apophis (Pravec et al., 2014).

The problem of shape reconstruction of a tumbler is essentially the same as in case of relaxed rotation. The only difference is that instead of four parameters describing the rotation state (the spin vector direction in ecliptic longitude and latitude, the angular frequency, and the initial orientation), we have now eight (three components of the angular momentum vector, three initial Euler angles, and two eigenvalues of the inertia tensor). Because the rotation P_ψ and precession P_ϕ periods can be estimated from the analysis of lightcurves, it is convenient to use them as parameters instead of the Euler angle θ_0 and the norm of the angular momentum vector L (Kaasalainen, 2001).

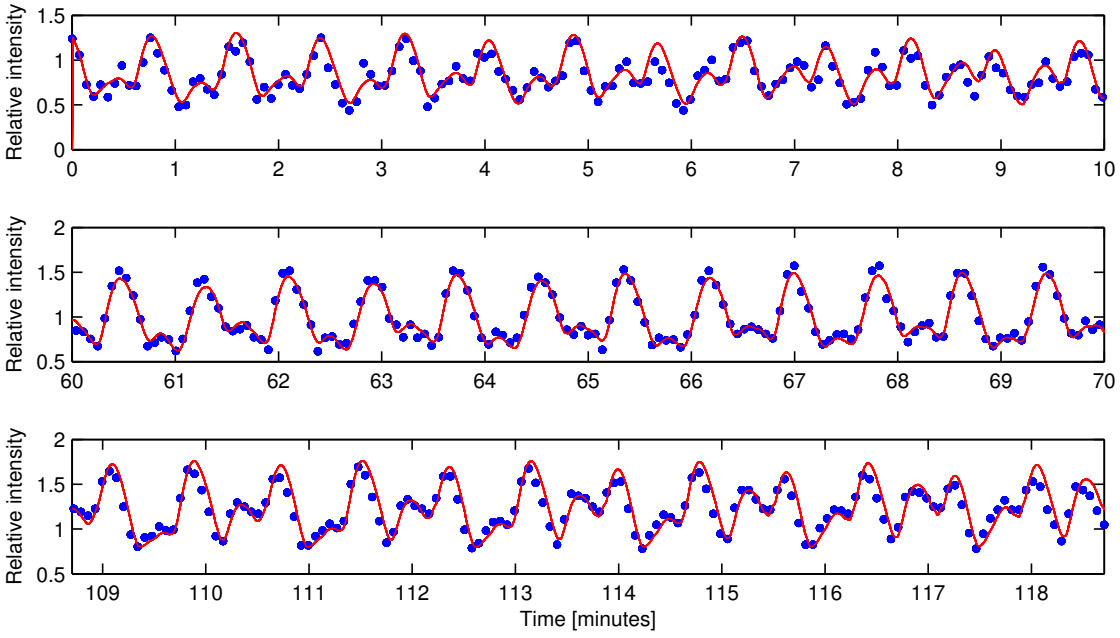

Figure 7: Photometric data of 2008 TC_3 (*blue points*) obtained in October 6/7, 2008 by Kozubal et al. (2011) and a synthetic lightcurve (*red*) based on our precessing shape model (Scheirich et al., 2010).

As an example, I show here model of asteroid 2008 TC_3. It was the first object for which an impact on Earth was predicted and then observed. It was discovered about twenty hours before it exploded in Earth's atmosphere. The asteroid was observed photometrically during two hours. The complicated pattern of its lightcurve (Fig. 7) revealed that the asteroid was tumbling. The Fourier analysis of the data show two periods $P_1 = 49.0338\,\mathrm{s}$ and $P_2 = 96.987\,\mathrm{s}$ (Fig. 8).

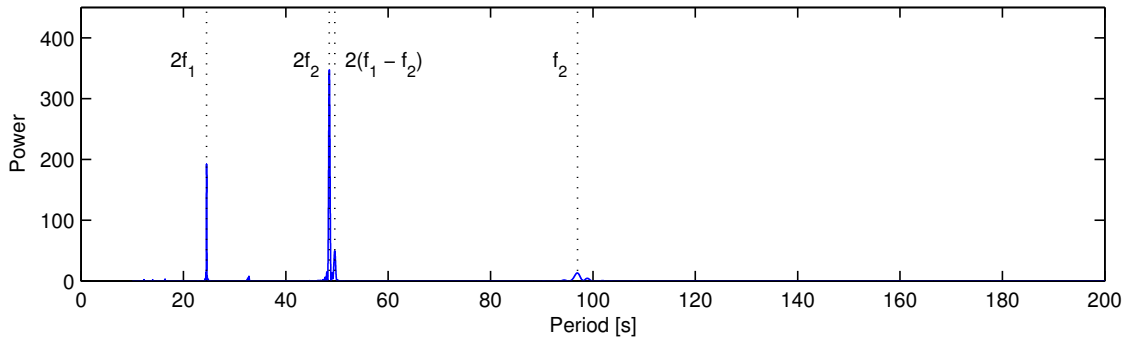

Figure 8: Lomb periodogram of photometric data of 2008 TC_3 (Fig. 7). The lightcurve can be modelled with two-period Fourier series with periods $P_1 = 1/f_1 = 49.0338\,\mathrm{s}$ and $P_2 = 1/f_2 = 96.987\,\mathrm{s}$. The strongest signal is at the frequency $2f_2$, other peaks are at frequencies $2f_1$, $2(f_1 - f_2)$, and f_2.

The model was derived by Scheirich et al. (2010). We found two mirror solutions of the shape and the direction of the angular momentum vector with the rotational and precession periods of 99.20 s and 97.00 s, respectively. The rotation corresponds to the long-axis mode and the apparent and physical periods are related as $1/P_1 = 1/P_\phi + 1/P_\psi$ and $P_2 = P_\phi$.

5.2 YORP

Apart from gravitation, there are various *non-gravitational forces* acting on small bodies in the solar system. For asteroids smaller than $\sim$ 40 km, their orbits and spin states can be affected by the solar radiation. A part of the solar radiation is scattered back to the space and is responsible for lightcurves in optical wavelengths. The rest of the incoming radiation is absorbed and heats the asteroid. In general, the distribution of temperature on asteroid's surface is not uniform. Infrared photons emitted from the surface carry out momentum and this leads to the recoil force and torque. The net force integrated over the surface is in general nonzero and causes acceleration or deceleration of the asteroid, which on long time scales leads to increasing or decreasing of the semimajor axis. This so called *Yarkovsky effect* has been recognized as the main transportation mechanism in the main belt (for review see Bottke et al., 2006; Vokrouhlický et al., 2015).

Yarkovsky effect is important for the orbital evolution. The *Yarkovsky-O'Keefe-Radzievskii-Paddack (YORP) effect* is more important for our purposes, because it is a net torque acting on asteroids with irregular shapes that in general changes their spin state. For a principal axis rotator, YORP changes both the spin axis direction and the rotation period. However, on a time scale of years, only the change in period can be detected from the analysis of lightcurves.

The change of the rotational period due to the YORP effect is usually very small and scales with the size D of an asteroid as $1/D^2$. Only for small asteroids, the change can be such that it is detectable by comparing synodic rotational periods measured in different apparitions, which was the case of asteroid (54509) YORP (Lowry et al., 2007). For kilometer-sized asteroids, YORP is weak and the uncertainty of periods from different apparitions is much larger than the change caused by YORP. In these cases, the only way how to detect changes in the rotational speed is to show that a constant-period model does not fit the data, while a YORP model does.

When including the YORP effect into the full inversion process, the rotational frequency $\omega = 2\pi/P$ is assumed to change linearly in time as

$$\omega(t) = \omega(t_0) + \upsilon(t - t_0)\,, \tag{1}$$

where $\upsilon = \mathrm{d}\omega/\mathrm{d}t$. In modelling, υ is another free parameter that has to be optimized. If the rotation rate changes linearly, the phase ϕ changes quadratically in time with respect to the

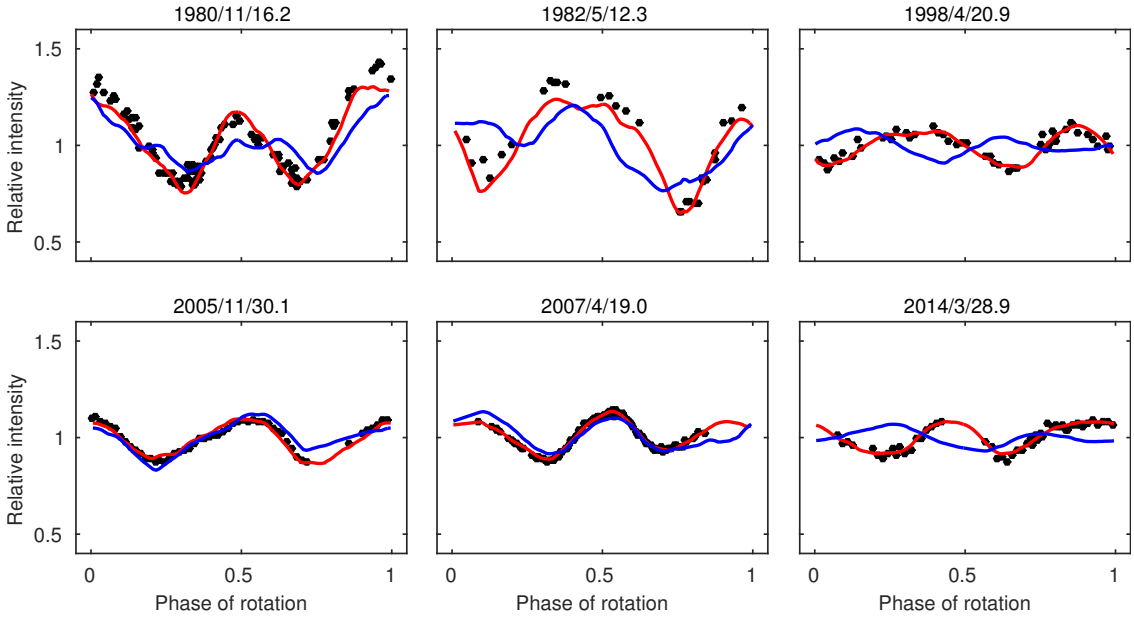

Figure 9: Example lightcurves of asteroid (1862) Apollo from six apparitions showing that the YORP model (*red*) gives an acceptable fit while the best constant-period model (*blue*) fails to fit the data.

constant rate $\omega(t_0)$ as

$$\delta\phi = \frac{1}{2}\upsilon(t - t_0)^2\,, \tag{2}$$

which makes even small changes of ω of the order of 10^{-8} rad d^{-2} detectable with data sets covering tens of years. However, the value $\omega(t_0)$ itself is a subject of optimization and the phase difference between models with $\upsilon \neq 0$ and $\upsilon = 0$ will be always smaller than the maximum value given by eq. (2). To reliably detect the YORP-induced change of the rotation period, we need to have many lightcurves covering a long interval of time. In such case, a constant period model and a YORP model significantly differ, the latter giving a better fit to the data as is shown in Fig. 9 for asteroid (1862) Apollo.

The first YORP detection was for asteroids (1862) Apollo (Kaasalainen et al., 2007; Ďurech et al., 2008) and (54509) YORP (Lowry et al., 2007; Taylor et al., 2007). Later, other detections for (1620) Geographos (Ďurech et al., 2008), (3103) Eger (Ďurech et al., 2012), and (25143) Itokawa (Lowry et al., 2014) have followed. What is interesting is that so far, only positive values of YORP have been detected. It is not clear if this is a selection effect, an unlikely realization, or a real physical effect caused perhaps by the tangential YORP (Golubov and Krugly, 2012; Golubov et al., 2014; Ševeček et al., 2015). Because YORP is an important dynamical process responsible for the distribution of rotation periods and spins of small asteroids (Pravec et al., 2008; Hanuš et al., 2013b) and for the creation of binaries and pairs (Pravec et al., 2010), other detections of YORP are of crucial importance for further progress in this field.

5.3 Binary asteroids

Binary asteroids are an essential part of the whole asteroidal population. According to Pravec et al. (2006), about one sixth of NEA population are binaries and a similar fraction is assumed also for small MBAs. In general, binary asteroids are complex systems with dynamical effects and complex geometry that complicate the inversion of their photometric data. Modelling of small binaries is a domain of radar observations (Ostro et al., 2006, for example). Here I focus on two cases where the complexity of a binary system is significantly reduced.

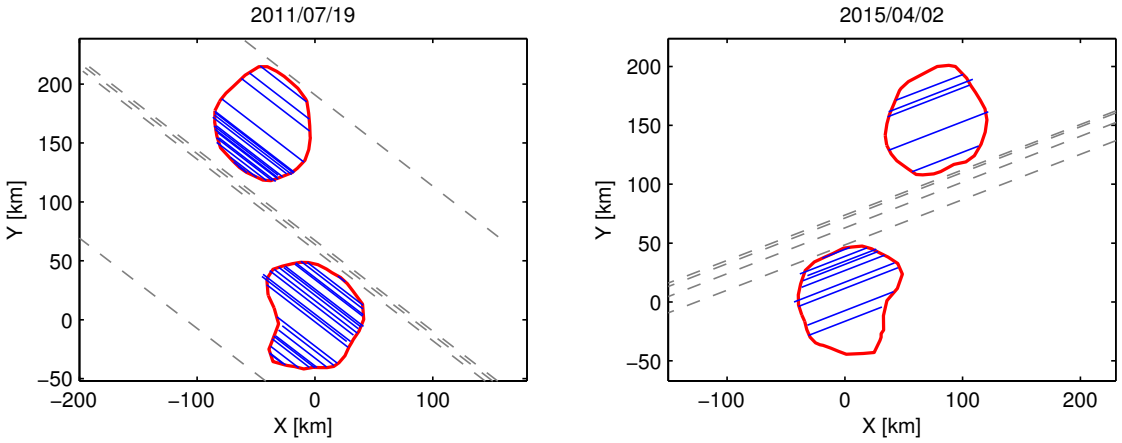

Figure 10: A comparison between the projection of the shape model (*red*) of binary asteroid (90) Antiope (Fig. 11) and occultation chords (*blue*). The dashed lines represent observers that reported no occultation.

Small secondaries There are binary asteroids for which their satellite (or more of them) is very small with respect to the main body. These satellites were discovered by adaptive-optics observations and their orbits were reconstructed from astrometric measurements (Descamps et al., 2008, for example). The satellites are so small that their photometric signal can be neglected with respect to the larger body. If there are lightcurves and AO data for the primary, its shape and spin can be reconstructed. The spin axis of the primary can be then compared with the orientation of the satellite orbital plane. We can also compare the quadrupole gravitational moment J_2 computed from the shape assuming uniform density and the value constrained by the orbit of the satellite. For example, for asteroid (87) Sylvia, the discrepancy between the nonzero shape-based J_2 and the null J_2 implied by the Keplerian orbits of two satellites can be interpreted as non-homogeneous mass distribution inside the primary (Berthier et al., 2014). We did a similar analysis also for Trojan asteroid (624) Hektor and its small satellite (Marchis et al., 2014).

Fully synchronous systems A substantial simplification in a description of a binary system occurs when the system if fully synchronous, i.e., when there is only one period in the system and the bodies are on a circular orbit. From the modelling point of view, such binaries are only extreme cases of a nonconvex model. Because the relative orientation of the two bodies is fixed, no additional parameters are needed – contrary to general asynchronous binary systems with eccentric orbits that have to be modelled with the mutual orbit taken into account (Scheirich and Pravec, 2009).

An example of a fully synchronous binary system is (90) Antiope, for which a lot of lightcurves have been observed (Michałowski et al., 2004). Although modelling of the system is possible from lightcurves only (Descamps et al., 2009), two stellar occultations observed in 2011 (Colas et al., 2012) and 2015 enabled us to robustly reconstruct the system (Figs. 10 and 11).

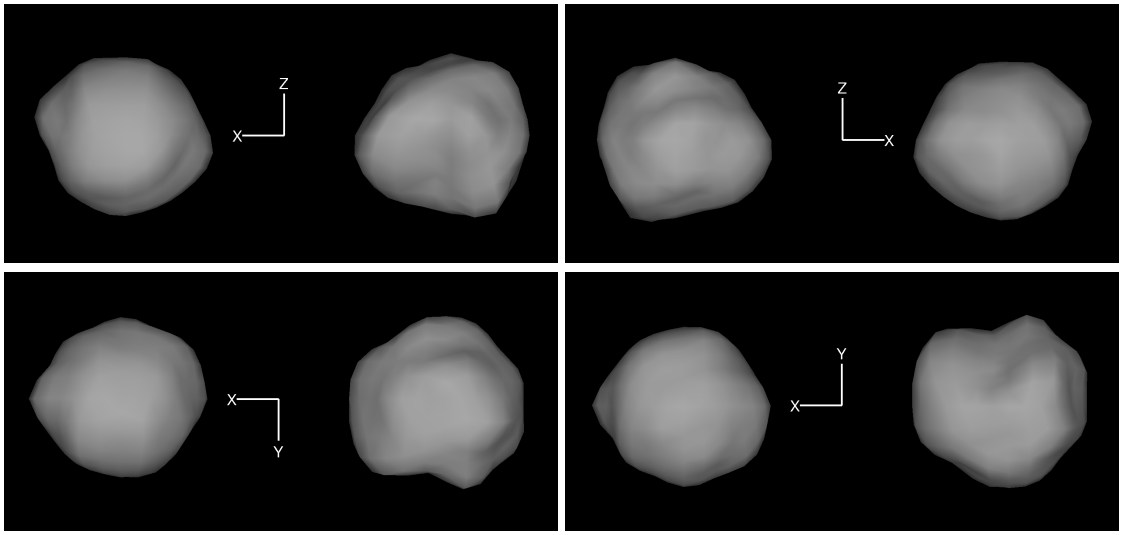

Figure 11: A shape model of (90) Antiope reconstructed from lightcurves and occultations (Fig. 10). The model is shown from four different directions, the mutual orbital plane is xy.

6 Future

Disk-resolved data with higher resolution will enable us to derive detailed models of selected asteroids, but photometric data will likely remain the main source of information for deriving low-resolution shape models and spin orientation. Classical lightcurves are now routinely observed by amateur observers, who publish their data in the Minor Planet Bulletin and share them through the ALCDEF database hosted by the Minor Planet Center.[4] Although the number of archived lightcurves is impressive, the dominant source of photometry in the next decade will be sparse photometry from surveys. We can expect a significant shift in both quality and quantity of sparse data. The shift in quality will come mainly with the release of Gaia data, the quantity of sparse data will continuously increase with the main breakthrough expected in 2020 with the Large Synoptic Survey Telescope start of operation. With big data flow, the critical points of inversion will be automated processing, validating and reliability test for the formally best-fit models. Because the combination of all available data is a must if we want to maximize the scientific output, correct weighting of various data sets is important. Of utmost importance is also debiasing the sample of shapes and spins. As shown by Marciniak et al. (2015), current data and models are biased against long-period low-amplitude models, which is especially true for models based on sparse data (Ďurech et al., 2016).

The availability of shape models and the data is essential for independent reliability checks and further interpretation of results and statistical analysis, for example. At present, most of the lightcurve-based models are available in the Database of Asteroid Models from Inversion Techniques (DAMIT)[5] (Ďurech et al., 2010). We plan to further develop its structure, continuously add new models when available, and maintain its reliability.

[4] http://www.minorplanetcenter.net/light_curve2/light_curve.php
[5] http://astro.troja.mff.cuni.cz/projects/asteroids3D

References

Alí-Lagoa, V., Lionni, L., Delbo, M., et al. (2014): Thermophysical properties of near-Earth asteroid (341843) 2008 EV_5 from WISE data. *Astron. Astrophys.* 561, A45.

André, C. L. F. (1901): Sur le système formé par la Planète double (433) Eros. *Astronomische Nachrichten* 155, 27–30.

Apostolovska, G., Donchev, Z., Kostov, A., et al. (2014): Photometry and shape modeling of Mars crosser asteroid (1011) Laodamia. *Serbian Astronomical Journal* 189, 79–85.

Berthier, J., Vachier, F., Marchis, F., Ďurech, J., and Carry, B. (2014): Physical and dynamical properties of the main belt triple Asteroid (87) Sylvia. *Icarus* 239, 118–130.

Bottke, W. F., Vokrouhlický, D., Walsh, K. J., et al. (2015): In search of the source of asteroid (101955) Bennu: Applications of the stochastic YORP model. *Icarus* 247, 191–217.

Bottke, W. F., Jr., Vokrouhlický, D., Rubincam, D. P., and Nesvorný, D. (2006): The Yarkovsky and Yorp effects: Implications for asteroid dynamics. *Annual Review of Earth and Planetary Sciences* 34, 157–191.

Bowell, E., Oszkiewicz, D. A., Wasserman, L. H., et al. (2014): Asteroid spin-axis longitudes from the Lowell Observatory database. *Meteoritics and Planetary Science* 49, 95–102.

Carry, B., Matter, A., Scheirich, P., et al. (2015): The small binary asteroid (939) Isberga. *Icarus* 248, 516–525.

Colas, F., Berthier, J., Vachier, F., et al. (2012): Shape and size of (90) Antiope derived from an exceptional stellar occultation on July 19, 2011. In *Asteroids, Comets, Meteors 2012*, volume 1667 of *LPI Contributions*, page 6427.

Connelly, R. and Ostro, S. J. (1984): Ellipsoids and lightcurves. *Geometriae Dedicata* 17, 87–98.

Delbo, M., Mueller, M., Emery, J. P., Rozitis, B., and Capria, M. T. (2015): Asteroid thermophysical modeling. In Michel, P., DeMeo, F. E., and Bottke, W. F., editors, *Asteroids IV*, pages 107–128. University of Arizona Press, Tucson.

Descamps, P., Marchis, F., Michalowski, T., et al. (2009): A giant crater on 90 Antiope? *Icarus* 203, 102–111.

Descamps, P., Marchis, F., Pollock, J., et al. (2008): 2007 Mutual events within the binary system of (22) Kalliope. *Planet. Space Sci.* 56, 1851–1856.

Ďurech, J., Grav, T., Jedicke, R., Kaasalainen, M., and Denneau, L. (2005): Asteroid models from the Pan-STARRS photometry. *Earth, Moon, and Planets* 97, 179–187.

Ďurech, J., Kaasalainen, M., Marciniak, A., et al. (2007): Physical models of ten asteroids from an observers' collaboration network. *Astron. Astrophys.* 465, 331–337.

Ďurech, J., Vokrouhlický, D., Kaasalainen, M., et al. (2008): New photometric observations of asteroid (1862) Apollo and (25143) Itokawa – an analysis of YORP effect. *Astron. Astrophys.* 488, 345–350.

Ďurech, J., Vokrouhlický, D., Kaasalainen, M., et al. (2008): Detection of the YORP effect in asteroid (1620) Geographos. *Astron. Astrophys.* 489, L25–L28.

Ďurech, J., Kaasalainen, M., Warner, B. D., et al. (2009): Asteroid models from combined sparse and dense photometric data. *Astron. Astrophys.* 493, 291–297.

Ďurech, J., Sidorin, V., and Kaasalainen, M. (2010): DAMIT: a database of asteroid models. *Astron. Astrophys.* 513, A46.

Ďurech, J., Kaasalainen, M., Herald, D., et al. (2011): Combining asteroid models derived by lightcurve inversion with asteroidal occultation silhouettes. *Icarus* 214, 652–670.

Ďurech, J., Delbo, M., and Carry, B. (2012): Asteroid models derived from thermal infrared data and optical lightcurves. *LPI Contributions* 1667, 6118.

Ďurech, J., Vokrouhlický, D., Baransky, A. R., et al. (2012): Analysis of the rotation period of asteroids (1865) Cerberus, (2100) Ra-Shalom, and (3103) Eger – search for the YORP effect. *Astron. Astrophys.* 547, A10.

Ďurech, J., Hanuš, J., and Vančo, R. (2015): Asteroids@home – A BOINC distributed computing project for asteroid shape reconstruction. *Astronomy and Computing* 13, 80–84.

Ďurech, J., Hanuš, J., Oszkiewicz, D., and Vančo, R. (2016): Asteroid models from the Lowell photometric database. *Astron. Astrophys.* 587, A48.

Ďurech, J., Hanuš, J., Alí-Lagoa, V. M., Delbo, M., and Oszkiewicz, D. A. (2016): WISE data and sparse photometry used for shape reconstruction of asteroids. In Chesley, S. R., Morbidelli, A., Jedicke, R., and Farnocchia, D., editors, *IAU Symposium*, volume 318 of *IAU Symposium*, pages 170–176.

Golubov, O. and Krugly, Y. N. (2012): Tangential component of the YORP effect. *Astrophys. J. Letters* 752, L11.

Golubov, O., Scheeres, D. J., and Krugly, Y. N. (2014): A three-dimensional model of tangential YORP. *Astrophys. J.* 794, 22.

Hanuš, J., Delbo, M., Ďurech, J., and Alí-Lagoa, V. (2015): Thermophysical modeling of asteroids from WISE thermal infrared data – Significance of the shape model and the pole orientation uncertainties. *Icarus* 256, 101–116.

Hanuš, J., Marchis, F., and Ďurech, J. (2013a): Sizes of main-belt asteroids by combining shape models and Keck adaptive optics observations. *Icarus* 226, 1045–1057.

Hanuš, J., Ďurech, J., Brož, M., et al. (2011): A study of asteroid pole-latitude distribution based on an extended set of shape models derived by the lightcurve inversion method. *Astron. Astrophys.* 530, A134.

Hanuš, J., Ďurech, J., Brož, M., et al. (2013b): Asteroids' physical models from combined dense and sparse photometry and scaling of the YORP effect by the observed obliquity distribution. *Astron. Astrophys.* 551, A67.

Hapke, B. (1981): Bidirectional reflectance spectroscopy. I – Theory. *J. Geophys. Res.* 86, 3039–3054.

Hapke, B. (1984): Bidirectional reflectance spectroscopy. III – Correction for macroscopic roughness. *Icarus* 59, 41–59.

Hapke, B. (1986): Bidirectional reflectance spectroscopy. IV – The extinction coefficient and the opposition effect. *Icarus* 67, 264–280.

Hestroffer, D., Tanga, P., Cellino, A., et al. (2002): Asteroids observations with the Hubble Space Telescope. I. Observing strategy, and data analysis and modeling process. *Astron. Astrophys.* 391, 1123–1132.

Hudson, R. S., Ostro, S. J., and Scheeres, D. J. (2003): High-resolution model of Asteroid 4179 Toutatis. *Icarus* 161, 346–355.

Johansen, A. and Lacerda, P. (2010): Prograde rotation of protoplanets by accretion of pebbles in a gaseous environment. *MNRAS* 404, 475–485.

Kaasalainen, M. (2001): Interpretation of lightcurves of precessing asteroids. *Astron. Astrophys.* 376, 302–309.

Kaasalainen, M. (2004): Physical models of large number of asteroids from calibrated photometry sparse in time. *Astron. Astrophys.* 422, L39–L42.

Kaasalainen, M. (2011): Maximum compatibility estimates and shape reconstruction with boundary curves and volumes of generalized projections. *Inverse Problems and Imaging* 5, 37–57.

Kaasalainen, M. and Ďurech, J. (2007): Inverse problems of NEO photometry: Imaging the NEO population. In Milani, A., Valsecchi, G. B., and Vokrouhlický, D., editors, *Near Earth Objects, our Celestial Neighbors: Opportunity and Risk*, page 151. Cambridge University Press, Cambridge.

Kaasalainen, M. and Ďurech, J. (2013): What's out there? Asteroid models for target selection and mission planning. In Badescu, V., editor, *Asteroids: Prospective Energy and Material Resources*, pages 131–150. Springer, Berlin.

Kaasalainen, M., Hestroffer, D., and Tanga, P. (2005): Physical models and refined orbits for asteroids from Gaia photometry and astrometry. In *ESA SP-576: The Three-Dimensional Universe with Gaia*, page 301.

Kaasalainen, M. and Lamberg, L. (2006): Inverse problems of generalized projection operators. *Inverse Problems* 22, 749–769.

Kaasalainen, M., Lamberg, L., and Lumme, K. (1992a): Interpretation of lightcurves of atmosphereless bodies. II – Practical aspects of inversion. *Astron. Astrophys.* 259, 333–340.

Kaasalainen, M., Lamberg, L., Lumme, K., and Bowell, E. (1992b): Interpretation of lightcurves of atmosphereless bodies. I – General theory and new inversion schemes. *Astron. Astrophys.* 259, 318–332.

Kaasalainen, M. and Torppa, J. (2001): Optimization methods for asteroid lightcurve inversion. I. Shape determination. *Icarus* 153, 24–36.

Kaasalainen, M., Torppa, J., and Muinonen, K. (2001): Optimization methods for asteroid lightcurve inversion. II. The complete inverse problem. *Icarus* 153, 37–51.

Kaasalainen, M., Ďurech, J., Warner, B. D., Krugly, Y. N., and Gaftonyuk, N. M. (2007): Acceleration of the rotation of asteroid 1862 Apollo by radiation torques. *Nature* 446, 420–422.

Keihm, S., Tosi, F., Kamp, L., et al. (2012): Interpretation of combined infrared, submillimeter, and millimeter thermal flux data obtained during the Rosetta fly-by of Asteroid (21) Lutetia. *Icarus* 221, 395–404.

Keller, H. U., Barbieri, C., Koschny, D., et al. (2010): E-Type asteroid (2867) Steins as imaged by OSIRIS on board Rosetta. *Science* 327, 190–.

Kozubal, M. J., Gasdia, F. W., Dantowitz, R. F., Scheirich, P., and Harris, A. W. (2011): Photometric observations of Earth-impacting asteroid 2008 TC_3. *Meteoritics and Planetary Science* 46, 534–542.

Kryszczyńska, A., La Spina, A., Paolicchi, P., et al. (2007): New findings on asteroid spin-vector distributions. *Icarus* 192, 223–237.

La Spina, A., Paolicchi, P., Kryszczyńska, A., and Pravec, P. (2004): Retrograde spins of near-Earth asteroids from the Yarkovsky effect. *Nature* 428, 400–401.

Lagerros, J. S. V. (1996): Thermal physics of asteroids. I. Effects of shape, heat conduction and beaming. *Astron. Astrophys.* 310, 1011–1020.

Lagerros, J. S. V. (1998): Thermal physics of asteroids. IV. Thermal infrared beaming. *Astron. Astrophys.* 332, 1123–1132.

Lowry, S. C., Fitzsimmons, A., Pravec, P., et al. (2007): Direct detection of the asteroidal YORP effect. *Science* 316, 272–274.

Lowry, S. C., Weissman, P. R., Duddy, S. R., et al. (2014): The internal structure of asteroid (25143) Itokawa as revealed by detection of YORP spin-up. *Astron. Astrophys.* 562, A48.

Magnusson, P., Barucci, M. A., Drummond, J. D., et al. (1989): Determination of pole orientations and shapes of asteroids. In Binzel, R. P., Gehrels, T., and Matthews, M. S., editors, *Asteroids II*, pages 66–97. University of Arizona Press, Tucson.

Mainzer, A., Bauer, J., Grav, T., et al. (2011): Preliminary results from NEOWISE: An enhancement to the Wide-field Infrared Survey Explorer for solar system science. *Astrophys. J.* 731, 53.

Marchis, F., Ďurech, J., Castillo-Rogez, J., et al. (2014): The puzzling mutual orbit of the binary Trojan asteroid (624) Hektor. *Astrophys. J. Letters* 783, L37.

Marchis, F., Kaasalainen, M., Hom, E. F. Y., et al. (2006): Shape, size and multiplicity of main-belt asteroids. *Icarus* 185, 39–63.

Marciniak, A., Michałowski, T., Polińska, M., et al. (2011): Photometry and models of selected main belt asteroids. VIII. Low-pole asteroids. *Astron. Astrophys.* 529, A107.

Marciniak, A., Pilcher, F., Oszkiewicz, D., et al. (2015): Against the biases in spins and shapes of asteroids. *Planet. Space Sci.* 118, 256–266.

Merline, W. J., Drummond, J. D., Carry, B., et al. (2013): The Resolved Asteroid Program – Size, shape, and pole of (52) Europa. *Icarus* 225, 794–805.

Michałowski, T., Bartczak, P., Velichko, F. P., et al. (2004): Eclipsing binary asteroid 90 Antiope. *Astron. Astrophys.* 423, 1159–1168.

Nortunen, H. and Kaasalainen, M. (2016): Shape and spin distribution of large object populations from random projection areas. *Inverse Problems and Imaging,* submitted.

Ostro, S. J. and Connelly, R. (1984): Convex profiles from asteroid lightcurves. *Icarus* 57, 443–463.

Ostro, S. J., Margot, J.-L., Benner, L. A. M., et al. (2006): Radar imaging of binary near-Earth asteroid (66391) 1999 KW4. *Science* 314, 1276–1280.

Polishook, D. (2014): Spin axes and shape models of asteroid pairs: Fingerprints of YORP and a path to the density of rubble piles. *Icarus* 241, 79–96.

Pravec, P., Harris, A. W., Vokrouhlický, D., et al. (2008): Spin rate distribution of small asteroids. *Icarus* 197, 497–504.

Pravec, P., Scheirich, P., Kušnirák, P., et al. (2006): Photometric survey of binary near-Earth asteroids. *Icarus* 181, 63–93.

Pravec, P., Scheirich, P., Ďurech, J., et al. (2014): The tumbling spin state of (99942) Apophis. *Icarus* 233, 48–60.

Pravec, P., Vokrouhlický, D., Polishook, D., et al. (2010): Formation of asteroid pairs by rotational fission. *Nature* 466, 1085–1088.

Rozitis, B., Maclennan, E., and Emery, J. P. (2014): Cohesive forces prevent the rotational breakup of rubble-pile asteroid (29075) 1950 DA. *Nature* 512, 174–176.

Russell, H. N. (1906): On the light variations of asteroids and satellites. *Astrophys. J.* 24, 1–18.

Santana-Ros, T., Bartczak, P., Michałowski, T., Tanga, P., and Cellino, A. (2015): Testing the inversion of asteroids' Gaia photometry combined with ground-based observations. *MNRAS* 450, 333–341.

Scheirich, P., Ďurech, J., Pravec, P., et al. (2010): The shape and rotation of asteroid 2008 TC_3. *Meteoritics and Planetary Science* 45, 1804–1811.

Scheirich, P. and Pravec, P. (2009): Modeling of lightcurves of binary asteroids. *Icarus* 200, 531–547.

Sierks, H., Lamy, P., Barbieri, C., et al. (2011): Images of asteroid 21 Lutetia: A remnant planetesimal from the early solar system. *Science* 334, 487.

Silva, J. S. and Lazzaro, D. (2015): Pole and shape of (1459) Magnya, the outer main belt basaltic asteroid. *Astron. Astrophys.* 580, A70.

Szabó, G. M. and Kiss, L. L. (2008): The shape distribution of asteroid families: Evidence for evolution driven by small impacts. *Icarus* 196, 135–143.

Tanga, P. and Delbo, M. (2007): Asteroid occultations today and tomorrow: toward the GAIA era. *Astron. Astrophys.* 474, 1015–1022.

Tanga, P., Hestroffer, D., Cellino, A., et al. (2003): Asteroid observations with the Hubble Space Telescope. II. Duplicity search and size measurements for 6 asteroids. *Astron. Astrophys.* 401, 733–741.

Taylor, P. A., Margot, J.-L., Vokrouhlický, D., et al. (2007): Spin rate of asteroid (54509) 2000 PH5 increasing due to the YORP effect. *Science* 316, 274.

Ševeček, P., Brož, M., Čapek, D., and Ďurech, J. (2015): The thermal emission from boulders on (25143) Itokawa and general implications for the YORP effect. *MNRAS* 450, 2104–2115.

Viikinkoski, M., Kaasalainen, M., and Ďurech, J. (2015a): ADAM: a general method for using various data types in asteroid reconstruction. *Astron. Astrophys.* 576, A8.

Viikinkoski, M., Kaasalainen, M., Ďurech, J., et al. (2015b): VLT/SPHERE- and ALMA-based shape reconstruction of asteroid (3) Juno. *Astron. Astrophys.* 581, L3.

Vokrouhlický, D., Bottke, W. F., Chesley, S. R., Scheeres, D. J., and Statler, T. S. (2015): The Yarkovsky and YORP effects. In Michel, P., DeMeo, F. E., and Bottke, W. F., editors, *Asteroids IV*, pages 509–531. University of Arizona Press, Tucson.

Vokrouhlický, D. and Nesvorný, D. (2008): Pairs of asteroids probably of a common origin. *Astron. J.* 136, 280–290.

Warner, B. D., Harris, A. W., and Pravec, P. (2009): The asteroid lightcurve database. *Icarus* 202, 134–146.

Wright, E. L., Eisenhardt, P. R. M., Mainzer, A. K., et al. (2010): The Wide-field Infrared Survey Explorer (WISE): Mission description and initial on-orbit performance. *Astron. J.* 140, 1868.

7 Selected publications

- Ďurech, J., Grav, T., Jedicke, R., et al. (2005): Asteroid models from the Pan-STARRS photometry. *Earth, Moon, and Planets* 97, 179–187. DOI: 10.1007/s11038-006-9084-8

  By realistic simulations, we showed the possibility of using sparse data from the Pan-STARRS project for asteroid shape reconstruction.

- Kaasalainen, M., Ďurech, J., Warner, B. D., et al. (2007): Acceleration of the rotation of asteroid 1862 Apollo by radiation torques. *Nature* 446, 420–422. DOI: 10.1038/nature05614

  One of the first two detections – together with asteroid (54509) YORP (Lowry et al., 2007; Taylor et al., 2007) – of the YORP effect. From the modelling of lightcurves from 1980–2005, we detected the acceleration of the rotation rate $(5.3 \pm 1.3) \times 10^{-8}\mathrm{rad\,d^{-2}}$.

- Ďurech, J., Scheirich, P., Kaasalainen, M., et al. (2007): Physical models of asteroid from sparse photometric data. In Milani, A., Valsecchi, G. B., and Vokrouhlický, D., editors, *Near Earth Objects, our Celestial Neighbors: Opportunity and Risk*, page 191. Cambridge University Press, Cambridge. DOI: 10.1017/S1743921307003225

  A review paper discussing the potential of sparse photometry for asteroid shape reconstruction.

- Ďurech, J., Kaasalainen, M., Marciniak, A., et al. (2007): Physical models of ten asteroids from an observers' collaboration network. *Astron. Astrophys.* 465, 331–337. DOI: 10.1051/0004-6361:20066347

  We used the lightcurve inversion method to derive shape models of ten asteroids. The data were obtained through collaboration with amateur observers.

- Ďurech, J., Vokrouhlický, D., Kaasalainen, M., et al. (2008): New photometric observations of asteroid (1862) Apollo and (25143) Itokawa – an analysis of YORP effect. *Astron. Astrophys.* 488, 345–350. DOI: 10.1051/0004-6361:200809663

  By including new lightcurves from 2007, we updated the shape and spin state model of asteroid Apollo. We also placed an upper limit on the YORP effect for asteroid Itokawa.

- Ďurech, J., Vokrouhlický, D., Kaasalainen, M., et al. (2008): Detection of the YORP effect in asteroid (1620) Geographos. *Astron. Astrophys.* 489, L25–L28.
  DOI: 10.1051/0004-6361:200810672

  The third detection of the YORP effect. By lightcurve inversion, we detected the rotation rate acceleration $(1.15 \pm 0.15) \times 10^{-8}\mathrm{rad\,d^{-2}}$.

- Ďurech, J., Kaasalainen, M., Warner, B. D., et al. (2009): Asteroid models from combined sparse and dense photometric data. *Astron. Astrophys.* 493, 291–297.
  DOI: 10.1051/0004-6361:200810393

  New shape models for 24 asteroids, pole ecliptic latitudes for other 18 asteroids. The models were reconstructed from combined dense and sparse photometric data.

- Ďurech, J., Sidorin, V., and Kaasalainen, M. (2010): DAMIT: a database of asteroid models. *Astron. Astrophys.* 513, A46. DOI: 10.1051/0004-6361/200912693

  An "official" introduction of the Database of Asteroid Models from Inversion Techniques with the description of its content and data format.

- Scheirich, P., Durech, J., Pravec, P., et al. (2010): The shape and rotation of asteroid 2008 TC_3. *Meteoritics and Planetary Science* 45,
  1804–1811. DOI: 10.1111/j.1945-5100.2010.01146.x

  By the method of Kaasalainen (2001), we reconstructed the shape and spin state model of asteroid 2008 TC_3 from its lightcurves. The asteroid was in an excited rotation state.

- Ďurech, J., Kaasalainen, M., Herald, D., et al. (2011): Combining asteroid models derived by lightcurve inversion with asteroidal occultation silhouettes. *Icarus* 214, 652–670. DOI: 10.1016/j.icarus.2011.03.016

  By scaling shape models of asteroids to fit the occultation data, we obtained refined models for 44 asteroids. The typical accuracy of the size was $\sim 10\%$.

- Ďurech, J., Vokrouhlický, D., Baransky, A. R., et al. (2012): Analysis of the rotation period of asteroids (1865) Cerberus, (2100) Ra-Shalom, and (3103) Eger – search for the YORP effect. *Astron. Astrophys.* 547, A10. DOI: 10.1051/0004-6361/201219396

  By inversion of lightcurves for these three asteroids, we detected an acceleration of the spin rate of asteroid Eger and apart from creating their shape models, we put upper limits for YORP effect for Ra-Shalom and Cerberus.

- Kaasalainen, M. and Ďurech, J. (2013): What's out there? Asteroid models for target selection and mission planning. In Badescu, V., editor, *Asteroids: Prospective Energy and Material Resources*, pages 131–150. Springer, Berlin. DOI: 10.1007/978-3-642-39244-3_5

  A review chapter summarizing the methods and potential of remote sensing techniques for modelling asteroids for results-oriented readers.

- Ďurech, J., Carry, B., Delbo, M., et al. (2015): Asteroid models from multiple data sources. In Michel, P., DeMeo, F. E., and Bottke, W. F., editors, *Asteroids IV*, pages 183–202. University of Arizona Press, Tucson. DOI: 10.2458/azu_uapress_9780816532131-ch010

  A decadal review of inversion methods for asteroid shape reconstruction from remote-sensing data for Asteroids IV book.

- Ďurech, J., Hanuš, J., and Vančo, R. (2015): Asteroids@home – A BOINC distributed computing project for asteroid shape reconstruction. *Astronomy and Computing* 13, 80–84. DOI: 10.1016/j.ascom.2015.09.004

  Presentation of the distributed computing Asteroids@home with a brief description of the lightcurve inversion method and technical details of the project.

- Ďurech, J., Hanuš, J., Oszkiewicz, D., and Vančo, R. (2016): Asteroid models from the Lowell photometric database. *Astron. Astrophys.* 587, A48. DOI: 10.1051/0004-6361/201527573

  From the analysis of Lowell photometric data of the first 100,000 numbered asteroids, we derived 328 new models. This almost doubled the number of available models. To scan the period parameter space through the use of convex shape models, we used the distributed computing project Asteroids@home.